A Very Fast Phase in the Refolding of Disulfide-Intact Ribonuclease A: Implications for the Refolding and Unfolding Pathways†

Walid A. Houry, David M. Rothwarf, and Harold A. Scheraga*

Baker Laboratory of Chemistry, Cornell University, Ithaca, New York 14853-1301

Received October 26, 1993; Revised Manuscript Received December 15, 1993®

ABSTRACT: The refolding and unfolding of disulfide-intact ribonuclease A has been studied by using single-jump and double-jump stopped-flow techniques. Absorbance and fluorescence detection methods were used to follow the kinetics. By appropriate choice of solution conditions (1.5 M guanidine hydrochloride, pH 3.0, at temperatures ≤15 °C) to slow the refolding process, a new very fast phase has been observed in addition to the usual fast and slow phases that involve the unfolded species U_f and U_s, respectively. Double-jump experiments consisting of an unfolding step at 4.2 M guanidine hydrochloride and pH 2.0 followed by a refolding step at 1.5 M guanidine hydrochloride and pH 3.0 were carried out to monitor the unfolding process. These experiments demonstrated that the new phase arises from a separate unfolded species, U_{vf}, which is present to the extent of about 6% in the equilibrium ensemble of unfolded protein at high guanidine hydrochloride concentration and low pH. A new model for the unfolding pathway and interconversion among unfolded species is proposed based on two independent isomerization processes. The equilibrium constants and activation energies obtained for each process suggest that they involve the isomerization of cis prolines. We propose that the isomerizations occur at the X–Pro peptide bonds of Pro 93 and 114. In the model, U_{vf} is the first species to form without isomerization at any cis X–Pro peptide bonds when the native protein is unfolded; U_f and U_s then form from U_{vf} through two independent isomerization processes. Both prolines are in the native (cis) conformation in U_{vf}. In U_f, Pro 114 is in a nonnative (trans) conformation while, in U_s, Pro 93 is in a nonnative (trans) conformation. The slow folding species, U_s, actually consists of (at least) two species: U_s^{α} with Pro 93 in a nonnative (trans) conformation and U_s^{β} with both Pro 93 and 114 in nonnative (trans) conformations. Finally, the kinetic data suggest that the presence of a nonnative trans conformation at the Tyr 92–Pro 93 peptide bond impedes the refolding rate of ribonuclease A much more than the presence of a nonnative trans conformation at the Asn 113–Pro 114 peptide bond.

The principles governing the folding and unfolding of proteins are not yet well understood. Although it is generally accepted that the amino acid sequence of a given protein predetermines its native structure (Anfinsen & Scheraga, 1975), it is not yet known how that sequence directs the protein to fold to its native state. In trying to understand how a protein folds, one attempts to describe the intermediates that form and the events that occur as the protein conformation evolves from a statistical coil in the unfolded state to a well-defined three-dimensional structure in the native state. Identifying the structure of these intermediates and the nature of these events is important in solving the protein-folding problem. However, the folding pathway is often complicated by the heterogeneity of the unfolded species. The unfolded species is usually a mixture of species that fold to the native conformation along sequential or parallel pathways with different refolding rates. Therefore, it is important to understand the nature of these unfolded species and the factors that cause them to refold at different rates through different pathways. In this paper, we attempt to draw a detailed picture of the unfolded species of disulfide-intact bovine pancreatic ribonuclease A (RNase A)[1] that accounts for the different phases observed by absorbance and fluorescence upon refolding and unfolding of the protein.

In the refolding kinetics of RNase A, three phases, which are believed to arise from three unfolded species, have generally been reported in the literature (Garel & Baldwin, 1975; Hagerman & Baldwin, 1976; Schmid, 1983; Lin & Brandts, 1983b; Mui et al., 1985). There are a fast folding species, U_f, which refolds with a time constant on the millisecond time scale, and (at least) two slow folding species, U_s^I and U_s^{II}, which refold with time constants on the order of tens to hundreds of seconds. Lin and Brandts (1987) have also suggested the presence of a third slow folding species. Each species is proposed to fold independently to the native conformation, which is considered to be a single well-defined species.

Brandts et al. (1975) first proposed that the heterogeneity of the unfolded species is due to the cis–trans isomerization of X–Pro peptide bonds. From studies on model peptides (Thomas & Williams, 1972; Wüthrich & Grathwohl, 1974; Dyson et al., 1988), it was shown that these bonds have an equilibrium distribution of 20–40% cis and 60–80% trans. RNase A has four proline residues in its amino acid sequence; namely, Pro 42, 93, 114, and 117. In the native state, Pro 93 and 114 form cis X–Pro peptide bonds, while Pro 42 and 117 form trans X–Pro peptide bonds (Richards & Wyckoff, 1971; Wlodawer & Sjölin, 1983). In the unfolded state, each X–Pro peptide bond is expected to exist in two different conformations (cis and trans), resulting in multiple unfolded species.

† This work was supported by Grant No. GM-14312 from the National Institute of General Medical Sciences of the National Institutes of Health. Support was also received from the National Foundation for Cancer Research.

* Author to whom correspondence should be addressed.

® Abstract published in *Advance ACS Abstracts,* February 1, 1994.

[1] Abbreviations used: RNase A, disulfide-intact bovine pancreatic ribonuclease A; MES, 2-(*N*-morpholino)ethanesulfonic acid; DCIP, 2,6-dichlorophenolindophenol sodium salt; GdnHCl, ultrapure guanidine hydrochloride.

0006-2960/94/0433-2516$04.50/0

The generally accepted unfolding model for RNase A is

$$N \xrightarrow{\text{fast}} U_f \overset{\text{slow}}{\rightleftharpoons} U_s^{I,II} \quad (1)$$

The fast phase is postulated to be a conformational unfolding step (Schmid & Baldwin, 1979a), while the slow phase is proposed to be a proline isomerization step (Nall et al., 1978; Schmid, 1982). However, this model does not explain the presence of the new species (U_{vf}) described below, and therefore, a new model is proposed in the Discussion section.

The generally accepted refolding model is

$$U_f \rightarrow N \quad 20\% \text{ of the amplitude, fast} \quad (2)$$

$$U_s^{II} \rightarrow I_1 \rightarrow I_N \rightarrow N \quad 60\text{–}70\% \text{ of the amplitude, slow} \quad (3)$$

$$U_s^{I} \rightarrow (I') \rightarrow N \quad 10\text{–}20\% \text{ of the amplitude, very slow} \quad (4)$$

It has been shown, by monitoring of inhibitor binding, that both the fast and slow refolding reactions yield native protein (Garel & Baldwin, 1973). Intermediates are generally well populated only under strongly refolding conditions at low temperatures in the presence of stabilizing salts. I_1 is an intermediate in which the NH protons are protected against exchange early in the folding of U_s^{II} (Schmid & Baldwin, 1979b; Kim & Baldwin, 1980; Brems & Baldwin, 1985; Udgaonkar & Baldwin, 1988, 1990), while I_N is a native-like intermediate which has been proposed to have a trans X–Pro 93 peptide bond (Cook et al., 1979; Schmid & Blaschek 1981; Schmid, 1983; Schmid, 1986). The intermediate (I′) has not been observed experimentally, but is postulated to form on the basis of a kinetic analysis of the data present in the literature (Mui et al., 1985). Lin and Brandts (1983c, 1984) have proposed an alternative refolding model in which no native-like intermediates with trans X–Pro 93 peptide bonds are populated.

As far as the nature of the unfolded species is concerned, very little is known about the origin of U_s^I because of its very small amplitude and its very slow refolding rate. On the other hand, a large number of studies have been carried out to explore the nature of U_s^{II}. By using double-jump techniques, Cook et al. (1979) have proposed that (at least) Pro 93 is in a nonnative trans conformation in U_s^{II} (for reviews see Jaenicke, 1987; Kim & Baldwin, 1990). This is now generally accepted on the basis of the refolding studies by Schmid and his group on homologous ribonucleases in which Pro 93 was conserved (Krebs et al., 1983; Schmid et al., 1986; Lang et al., 1986; Lang & Schmid, 1990). Their studies demonstrated that all of these homologous proteins had refolding kinetics similar to those of bovine RNase A, and that U_s^{II} folded through a native-like intermediate I_N under strongly refolding conditions. Mutants of Pro 93 and 114 (Schultz & Baldwin, 1992; Schultz et al., 1992) showed unexpectedly complex kinetics so that, on the basis of these mutants, the role of Pro 93 in the refolding of the slow phase could not be simply explained. A mutant of Pro 42 has recently been studied in our laboratory (Dodge et al., 1994), and its refolding kinetics are similar to those of the native protein when monitored by absorbance, indicating that the cis–trans isomerization of Pro 42 does not contribute to the experimentally observed heterogeneity of the unfolded species.

The fast folding species, U_f, is not as well characterized as U_s^{II}. It has been regarded as an unfolded state in which all the prolines are in the native conformation. However, Henkens et al. (1980) have proposed that U_f contains a nonnative proline isomer. The authors argued that, if an X–Pro peptide bond has ~25% probability of adopting a cis conformation in the unfolded state of a protein and if U_f has two cis X–Pro peptide bonds, then its refolding amplitude should be about 0.25 × 0.25 = 6.25%, which is much lower than the experimental value of ~20%. Therefore, the authors concluded that U_f must contain a nonnative proline isomer.

In an effort to provide a further understanding of the nature of the unfolded state and to characterize U_f, we have carried out refolding studies under conditions in which the folding process has been slowed down so that the refolding phase involving U_f occurs on a time scale of seconds. These conditions were achieved by varying the GdnHCl concentration and by lowering the pH. However, the surprising result obtained here was the appearance of a new phase with a time constant on the order of milliseconds while the fast phase, under these refolding conditions, has a time constant on the order of seconds. We have labeled the species giving rise to this new phase as U_{vf} (for very fast). Furthermore, double-jump experiments were used to monitor the formation of the different unfolded species. From these experiments, a new picture emerges for the unfolding pathway and for the interconversion among the different unfolded species of RNase A. The implications of these results for the refolding pathways will be discussed.

MATERIALS AND METHODS

Reagents. Glycine, 2-(*N*-morpholino)ethanesulfonic acid (MES), L-ascorbic acid sodium salt, 2,6-dichlorophenolindophenol sodium salt (DCIP), and L-tyrosine were purchased from Sigma Chemical Company. NaCl, NaOH, HCl, acetic acid, and Na_2EDTA were obtained from Fisher Scientific Co. Guanidine hydrochloride (GdnHCl), ultra pure, was obtained from ICN Biochemicals and citric acid from Pierce Chemical Company.

Purification. RNase A, types I-A and II-A, was purchased from Sigma and was purified by cation-exchange chromatography according to the procedure of Rothwarf & Scheraga (1993). The purity of the protein was checked by using an analytical Bakerbond WP CBX column (J. T. Baker) or a Hydropore-5-SCX column (Rainin) on an 8700 Spectra-Physics HPLC apparatus. The protein was found to be >99% pure.

Buffer Characterization. GdnHCl concentration was determined by refractive index at 25 °C (Nozaki, 1972) using a Bausch & Lomb refractometer. The pH of the buffers (acetic acid, citric acid, Gly, and MES) was adjusted at room temperature using concentrated HCl or NaOH. It was found that the pH of the different buffers used changed with temperature by about 0.05–0.1 pH units/5 °C (see also Good & Izawa, 1972).

Thermal Transition. RNase A was dissolved in a buffer of 1.5 M GdnHCl, 38.1 mM Gly, 2.4 mM MES, and pH of 3.00 (±0.05). The pH of the sample did not change when measured at the end of the experiment. These conditions correspond to those used for refolding in the kinetic experiments described below. The concentration of the protein was 0.69 mg/mL as determined by absorbance at 277.5 nm (ϵ = 9800 M^{-1} cm^{-1}) (Sela & Anfinsen, 1957). A modified Cary model 14 spectrophotometer (Denton et al., 1982) was used to follow the absorbance change of the solution at 287 nm. A Hellma quartz cuvette with a 1.0-cm path length was used. The cuvette was placed in a cell holder thermostated by using a Neslab RTE-100 circulating bath controlled through a Sun IPC Sparcstation. A second cuvette filled with the appropriate buffer was placed in the cell holder, and a calibrated thermistor was placed in it. Temperature was determined to within 0.1

°C. The sample was allowed to equilibrate for 10–15 min at each temperature reading. Reversibility of the transition was checked by heating the sample and then cooling it.

Instrument Used for the Kinetic Measurements. A Hi-Tech Scientific PQ/SF-53 stopped-flow instrument was used for the kinetic measurements. A Keithley System 570 A/D box was used to convert the analogue signal obtained from the optical detector to a digital signal, which, in turn, was sent to a CompuAdd 286 computer. Soft500 software (Keithley) was used to collect the data, which were then transferred to an IPC Sun Sparcstation for further processing. Signals were collected at intervals of either 0.5 or 50 ms/point. A 50-W, 12-V halogen lamp was used for visible measurements; a 30-W Cathodeon deuterium lamp type B01 from Hellma Cells, Inc., was used for UV measurements; and a 75-W xenon arc lamp from Ushio Inc. Japan was used for fluorescence measurements. The xenon lamp was connected to a Kepco, Inc., power supply and a Schoeffel Instrument Corp. starter. The flow system was thermostated by using a Forma Scientific, Inc., circulating bath connected to a Little Giant Corp. pump. The temperature of the system was monitored by an internal thermistor placed next to the flow cell. The reading of the thermistor was checked against the reading of another external thermistor (Fisher Scientific Co.). Both thermistors gave the same reading within 0.2 °C.

The high-pressure distribution valves and check valves that were used for the flow circuit were purchased from Omnifit USA. Other fittings and tubings were obtained from Omnifit USA, Supelco, and Upchurch Scientific. The arrangement of the flow system for double-jump experiments was modified to minimize mixing artifacts by inserting check valves between the two syringes used in the first jump and the first mixer, and also between the flow cell and the stopping syringe. Syringes are driven pneumatically, and the pressure applied was typically 45 psi for single jumps and 80 psi for double jumps. High pressures resulted in wavy decay curves. This problem was solved by using larger diameter tubing going into the flow cell, which helped in dissipating the pressure wave created. Different mixing ratios in the instrument were achieved by using different size Hamilton syringes.

The linearity of the optical detection system used in the stopped-flow instrument was checked by measuring the absorbance of different tyrosine solutions of known concentrations at 274 nm. The concentrations of the tyrosine solutions were predetermined by measuring their absorbance on the modified Cary model 14 spectrophotometer. The optical system was found to be linear between 0 and 0.8 absorbance units, which is within the absorbance range measured during the kinetic runs. The instrument base line was stable with minimal drift for 15 min.

The monochromator used had a nominal dispersion of 7 nm/mm. The slit width for the absorbance measurements was adjusted to 1 mm with the wavelength set at 287 nm. The path length used was 10 mm. For the fluorescence refolding measurements, a slit width of 5 mm was used. However, for the unfolding measurements monitored by fluorescence, the slit width had to be reduced to 0.5 mm in order to minimize a photooxidation effect that was observed to occur in the unfolded protein. The excitation wavelength was set at 268 nm, the isosbestic point of RNase A (Schmid, 1981). The excitation path length was 10 mm, and the emission path length was 2 mm. A band-pass filter (280–400 nm) was placed between the photomultiplier tube and the flow cell during the fluorescence measurements.

Kinetic Experiments. Single-jump unfolding experiments were carried out at 4.2 M GdnHCl, pH 2.0, by mixing 1 volume of the folded protein in 1.5 M GdnHCl, 50 mM MES, pH 5.9, with 10 volumes of 4.47 M GdnHCl, 40 mM Gly, pH 1.8. Single-jump refolding experiments were carried out at 1.5 M GdnHCl, pH 3.0, by mixing 1 volume of unfolded protein in 4.2 M GdnHCl, 28.6 mM Gly, 14.3 mM MES, pH 2.3, with 5 volumes of 0.96 M GdnHCl, 40 mM Gly, pH 3.2. Double-jump experiments involved two steps. The first step was unfolding at 4.2 M GdnHCl, pH 2.0, achieved by mixing 1 volume of 1.5 M GdnHCl, 50 mM MES, pH 5.8, containing the folded protein with 2.5 volumes of 5.28 M GdnHCl, 40 mM Gly, pH 1.40. After a set delay time, which will be referred to later as the unfolding time, the second step was initiated; it was a refolding step carried out at 1.5 M GdnHCl, pH 3.0, by mixing 1 volume of the unfolded protein in 4.2 M GdnHCl, pH 2.0, from the first step with 5 volumes of 0.96 M GdnHCl, 50 mM citric acid buffer, pH 3.2. Samples were allowed to equilibrate for 20–30 min at the set temperature before starting the experiments. The kinetic runs were repeated 6 to 10 times for single-jump experiments and four to five times for double-jump experiments. Mixing artifacts usually persisted up to $\sim$10 ms. Final protein concentration in the flow cell was typically 0.7–1.0 mg/mL. However, for the unfolding experiments monitored by fluorescence, the protein concentration was 0.3 mg/mL.

Test Reaction for the Stopped-Flow Instrument. The reaction between DCIP and L-ascorbic acid (Tonomura et al., 1978) was used to determine the performance limits of the instrument and also to measure the volume of the line between the two mixers for the double-jump experiments. L-Ascorbic acid reduces DCIP, and the reaction is pseudo-first-order when ascorbic acid is present in large excess. The disappearance of the color of DCIP was followed at 524 nm, the isosbestic point of DCIP (Armstrong, 1964). A mixing ratio of 1:1 was used, and the final pH of the mixture was 2.1, with the temperature set at 19 °C. All solutions contained 0.2 M NaCl to minimize the effect of changes in ionic strength. The initial concentration of DCIP was fixed at 0.1 mM while the initial concentration of ascorbic acid was varied from 1 to 30 mM.

The plot of the pseudo-first-order rate constant, k(app), versus ascorbic acid concentration was linear from 1 to 10 mM ascorbic acid concentration (where the rate constant is 600 s^{-1}) and deviates from linearity above that range. The dead time of the instrument was calculated to be 2.1($\pm$0.2) ms, which is small compared to the time constants obtained in the kinetic experiments (ranging from 35 ms to hundreds of seconds) and, therefore, was not taken into account in fitting the data. Using the same procedure, a volume of 83($\pm$3) μL for the delay line between the two mixers was obtained. This volume was taken into account in calculating the delay times for the double-jump experiments.

Fitting the Data. The decay curves were fitted by using the program PLOT from New Unit (Ithaca, NY). The program utilizes a Levenberg–Marquardt algorithm (Marquardt, 1963) for nonlinear least squares fitting. Decay curves from the single-jump unfolding and refolding experiments were fitted to single or double exponentials to obtain the amplitudes and time constants. In fitting the refolding decay curves from the double-jump experiments, all amplitudes and time constants were allowed to vary except for the time constant of the slow phase, which was fixed at the value obtained from the single-jump experiments. The standard deviations for the amplitudes and the time constants were obtained in the usual way by calculating $[(\sum(y-\bar{y})^2)/(n-1)]^{1/2}$, where y is the experimental

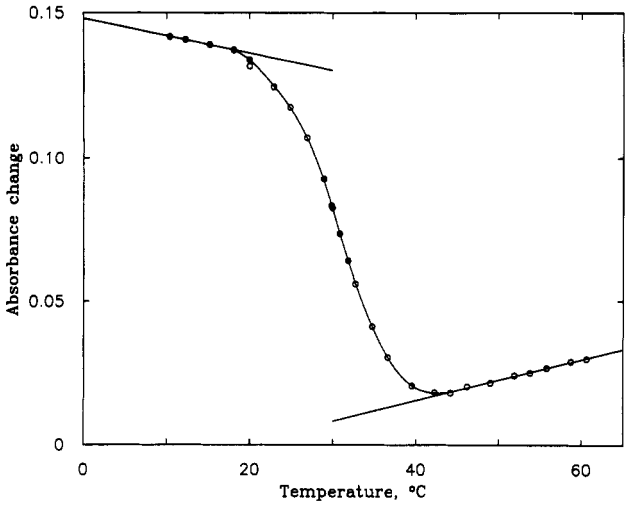

FIGURE 1: Thermal transition curve of RNase A (0.69 mg/mL) in 1.5 M GdnHCl, 38.1 mM Gly, 2.4 mM MES, and pH 3.0, measured by absorbance at 287 nm. T_m = 31.2 °C: (○) heating; (●) cooling. The straight lines are linear fits to the pretransition and posttransition regions.

value of the amplitude or time constant, $\bar{y}$ is the average value, and n is the number of repeated runs. All errors are listed at the 95% confidence limit.

The rate constants of the kinetic model proposed for the interconversion among unfolded species were calculated with the aid of a program written in this laboratory which uses a Runge–Kutta algorithm followed by a Simplex algorithm (Nelder & Mead, 1965; Caceci & Cacheris, 1984) to obtain a best fit to the experimental points. These points are the refolding amplitudes from the double-jump experiments monitored by absorbance at different unfolding times. The standard deviations for the rate constants of the kinetic model were obtained from a Monte Carlo procedure (Straume & Johnson, 1992). In this procedure, data sets consisting of theoretical amplitudes are created by adding to each experimental amplitude random Gaussian noise that has a standard deviation equal to the experimentally determined standard deviation of that amplitude; 2500 such theoretical data sets were created and fitted using the algorithm described above to obtain a Gaussian distribution of rate constants. The resulting rate constants were then averaged and their standard deviations calculated. The errors are given at the 95% confidence limit.

The treatment of the double-jump data monitored by fluorescence is presented in the Discussion section.

RESULTS

Thermal Transitions. Refolding of RNase A was carried out at 1.5 M GdnHCl, pH 3.0, and the thermal transition curve (Figure 1) was obtained under these conditions. The transition midpoint is 31.2(±0.2) °C, and the transition region extends from ~19 to 43 °C. Since the protein is folded at temperatures below 19 °C, all the temperatures used for the kinetic experiments were less than this value, i.e., 15, 11.8, 10, and 5 °C.

Single-Jump Unfolding Experiments. The unfolding reaction was followed by absorbance at 287 nm and by fluorescence using an excitation wavelength of 268 nm (Figure 2). The protein was unfolded at 4.2 M GdnHCl, pH 2.0. Only one phase was observed by absorbance with a temperature-dependent time constant ranging from 35 to 114 ms (Table 1). The unfolding experiments were repeated for a series of temperatures to obtain an activation energy of 19 kcal/mol for the observed relaxation (Table 1). Lin and Brandts (1983b) reported a value of 11 kcal/mol for the activation energy, but they used urea rather than GdnHCl. Since urea is less viscous than GdnHCl, the difference in the activation energies for the (conformational) unfolding could be due to the difference in the viscosities of the solutions used. Also, GdnHCl is a charged salt while urea is neutral and, therefore, the two denaturants would be expected to act differently to induce the unfolding of the protein.

By fluorescence, two phases were observed (Figure 2B,C): a fast phase and a slow phase. The fast phase appears to be the same as the phase observed by absorbance because of the similarities in the time constants of the two phases at the

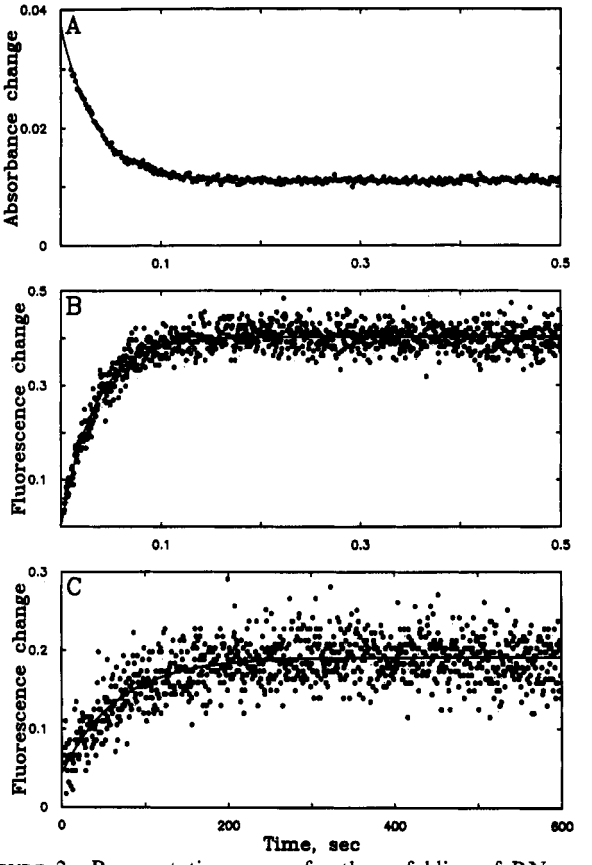

FIGURE 2: Reprsentative curves for the unfolding of RNase A. Unfolding was from 1.5 M GdnHCl, pH 5.9 to 4.2 M GdnHCl, pH 2.0, at 15 °C using the appropriate buffers. The final protein concentrations were 1.0 mg/mL for absorbance measurements and 0.3 mg/mL for fluorescence measurements. The solid lines are single exponential fits. When unfolding was followed by absorbance, only a fast phase (A) was detected. However, when unfolding was followed by fluorescence, a fast phase (B) and a slow (C) phase were detected.

Table 1: Temperature Dependence for the Single-Jump Unfolding Experiments[a]

	fast phase, τ (ms)		slow phase, τ (s)
temp (°C)	absorbance	fluorescence[b]	fluorescence[b]
15.0	35.0(1.6)	33.0(3.2)	69.8(10.5)
11.8	51.2(1.1)	47.8(3.7)	112.1(8.8)
10.0	61.2(1.4)	57.5(1.0)	138.5(6.8)
5.0	113.7(4.6)	100.0(5.0)	265.0(21.5)
E_a (kcal/mol)[c]	18.7(1.9)	17.6(1.3)	21.0(3.0)

[a] Unfolding was achieved by 1:10 dilution from 1.5 M GdnHCl, pH 5.9, to 4.2 M GdnHCl, pH 2.0. τ represents the average time constant. The final protein concentrations were 1.0 mg/mL for absorbance unfolding and 0.3 mg/mL for fluorescence unfolding. The numbers in parentheses give the errors at the 95% confidence limit. [b] By fluorescence: amplitude of fast phase/amplitude of slow phase = 75/25. [c] E_a is the activation energy of the rate constants (τ^{-1}).

Table 2: Results of the Single-Jump Refolding Experiments at 15 °C[a]

method of obsn	τ_{vf} (ms)	τ_f (s)	τ_s (s)	α_{vf}	α_f	α_s
absorbance	47.8(5.9)	3.85(0.36)	303(25)	6.1(1.5)	18.0(0.3)	75.9(1.8)
fluorescence	71.9(30.3)	6.15(1.73)	341(26)	1.7(1.7)	11.3(3.5)	87.0(5.9)

[a] Refolding was achieved by 1:5 dilution from 4.2 M GdnHCl, pH 2.3, to 1.5 M GdnHCl, pH 3.0. τ represents the average time constant, and α represents the average relative amplitude. The final protein concentration was 0.8 mg/mL. Subscripts vf, f, and s correspond to the very fast, fast, and slow phases, respectively. The amplitudes are normalized so that $\alpha_{vf} + \alpha_f + \alpha_s = 100$. The numbers in parentheses give the errors at the 95% confidence limit.

different temperatures (Table 1). The very slight differences that exist between the fluorescence and absorbance time constants at 10 and 5 °C, which do not overlap at the 95% confidence limit, are more likely due to some minor systematic errors that were not taken into account when fitting the data than due to any difference in the processes being monitored by the two optical techniques. The fluorescence fast phase has the same activation energy as that of the absorbance phase. The second phase observed by fluorescence is much slower with a smaller amplitude. The activation energy observed for the slower phase is 21 kcal/mol, and the relative amplitudes of the fast to slow phases is found to be 75:25 (Table 1). These results are similar to those reported by Rehage & Schmid (1982).

In following the unfolding experiments by fluorescence, an irreversible photooxidation effect, which resulted in a downward drift of the unfolding curve with time, occurred. The effect was minimized by defocusing the light from the xenon lamp and by narrowing the slit width of the monochromator thereby reducing the light intensity reaching the flow cell.

Single-Jump Refolding. The initial refolding experiments were carried out at a final concentration of 1.5 M GdnHCl, pH 3.0 and 15 °C. Refolding was followed by absorbance and fluorescence (Table 2 and Figures 3 and 4). Under these conditions, the new very fast phase can clearly be seen in Figures 3A (by absorbance) and 4A (by fluorescence). In the absorbance measurements, the very fast phase (species U_{vf}) has an amplitude of 6% with a time constant of 48 ms. The fast phase (species U_f) has an amplitude of 18% with a time constant of 4 s. Under the conditions of our experiments, the slow phases appear as a single phase, which is in agreement with observations reported in the literature (Schmid, 1983) for the refolding of RNase A at high GdnHCl concentrations. Hence, the slow phase (species U_s) can be considered as the sum of U_s^I and U_s^{II}, which correspond to the minor and major slow folding species observed under strongly native folding conditions. The slow phase has an amplitude of 76% and a time constant of 300 s.

The fluorescence experiments are in agreement with the absorbance results. The time constants of the three phases observed by fluorescence can be considered to be the same as the time constants of the phases seen by absorbance (Table 2). The slight difference between the absorbance and fluorescence time constants of U_f, which do not overlap at the 95% confidence limit, most likely arises from some systematic error in the fitting of the fluorescence data (due to both its small amplitude and low signal-to-noise ratio). The amplitudes obtained by fluorescence are different from those obtained by absorbance, possibly because each phase has a different quantum yield or because the refolding process observed by fluorescence is different from that observed by absorbance. In this paper, we use the former explanation in discussing the fluorescence data. This issue is explored further by the double-jump experiments.

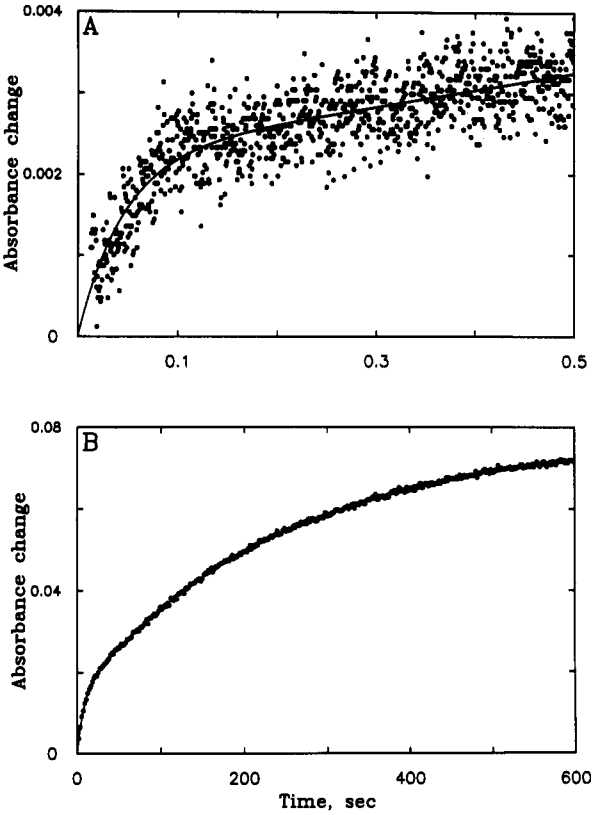

FIGURE 3: Representative curves for the refolding of RNase A when monitored by absorbance. Refolding was from 4.2 M GdnHCl, pH 2.3, to 1.5 M GdnHCl, pH 3.0, at 15 °C using the appropriate buffers. The solid lines are double exponential fits. Panel A shows mainly the refolding of U_{vf} with a contribution (the later slow rise) from the refolding of U_f. Panel B shows the refolding of an early fast phase corresponding to U_f and a later slower phase corresponding to U_s. The protein concentration (0.8 mg/mL) was the same in panels A and B.

Table 3: Temperature Dependence for the Single-Jump Refolding Experiments When Followed by Absorbance[a]

temp (°C)	τ_f (s)	τ_s (s)	α_f	α_s
15.0[b]	3.85(0.36)	303(25)	19.2(0.3)	80.8(1.9)
11.8	4.46(0.31)	456(22)	17.5(1.2)	82.5(2.1)
10.0	4.77(0.46)	535(18)	18.7(1.3)	81.3(5.7)
5.0	5.57(0.43)	840(169)	23.3(2.1)	76.7(12.3)
E_a (kcal/mol)[c]	5.8(4.5)	15.9(4.0)		

[a] Conditions and abbreviations are the same as in Table 2. α represents the relative absorbance amplitude. Only the fast and slow phases are listed (refer to Tables 2 and 4 for the very fast phase). Amplitudes are normalized so that $\alpha_f + \alpha_s = 100$. [b] Values at 15 °C are obtained from Table 2. However, it should be noted that the amplitudes were renormalized as indicated in footnote a. [c] E_a is the activation energy of the rate constants.

The refolding experiments were repeated at different temperatures to obtain the activation energy for each process (Table 3). The experiments were monitored by absorbance. The activation energy obtained for the refolding of U_f is 6 kcal/mol and for U_s is 16 kcal/mol. These values are similar to those reported in the literature (Schmid & Baldwin, 1978; Lin & Brandts, 1983b). When these experiments were carried out at temperatures below 15 °C, it was more difficult to observe the refolding of U_{vf} because of the mixing artifacts, which persisted for longer times. Hence, the activation energy for U_{vf} was determined more accurately from the double-jump experiments described below.

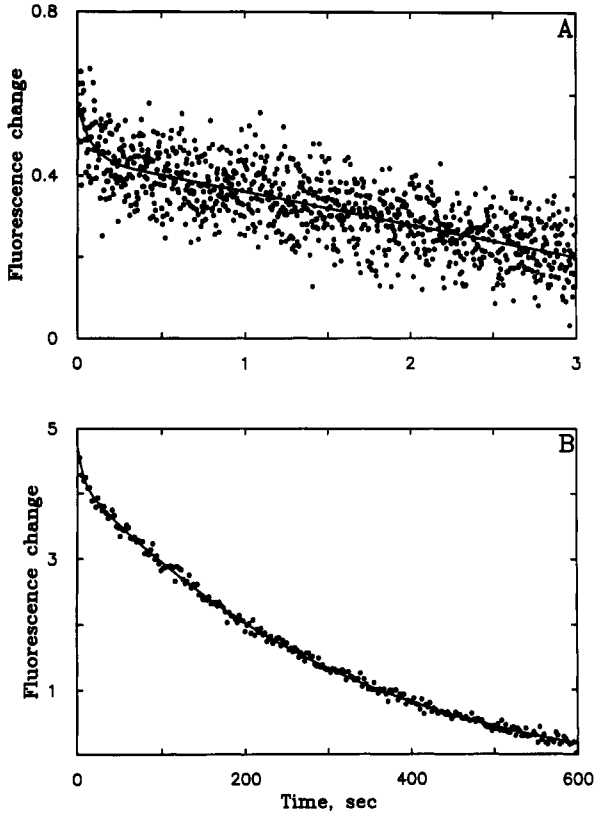

FIGURE 4: Representative curves for the refolding of RNase A when monitored by fluorescence. Refolding conditions are the same as those of Figure 3. Panel A shows mainly the refolding of U_{vf} with a contribution (the later slow decay) from the refolding of U_f. Panel B shows the refolding of an early fast phase corresponding to U_f and a later slower phase corresponding to U_s. The protein concentration (0.8 mg/mL) was the same in panels A and B.

Double-Jump Experiments. To provide further understanding of the nature of the newly observed very fast phase and its relation to the other unfolded species, double-jump experiments were carried out at different temperatures. These experiments enabled us to populate U_{vf} selectively and, also, to monitor the formation of the different unfolded species upon unfolding the protein. The experiments involved two steps: an unfolding step followed, after a certain delay time, by a refolding step. The delay time between the two steps will, henceforth, be referred to as the unfolding time. Only the refolding step is monitored optically, and the amplitudes obtained from fitting the refolding curves are a measure of the amount of U_{vf}, U_f, or U_s present in the unfolded state of the protein at that given unfolding time (or, correspondingly, at zero refolding time).

In the first series of experiments, the protein was first unfolded at 4.2 M GdnHCl, pH 2.0, and then was refolded at 1.5 M GdnHCl, pH 3.0, at temperatures of 15 °C and below, as indicated in Table 4. The refolding process was observed by absorbance. The unfolding time for this set of experiments was fixed at 1 s. At this unfolding time, the major phase was the very fast phase, and its activation energy was found to be 5 kcal/mol. Hence, the refolding activation energies for the three phases are 5, 6, and 16 kcal/mol for U_{vf}, U_f, and U_s, respectively. The significance of these values is presented in the Discussion section.

At this point, a question arises as to whether the protein is completely unfolded at 4.2 M GdnHCl, pH 2.0 and temperatures ≤15 °C, or whether there is some residual native-like structure present under these conditions. If native-like structure is present, U_{vf} would be the likely species to contain

Table 4: Temperature Dependence for the Refolding of U_{vf} by Double-Jump Experiments When Followed by Absorbance

temp (°C)	τ_{vf}[a] (ms)	τ_{vf}[b] (ms)
15.0	38.1(1.0)	35.0(3.8)
11.8	38.7(5.1)	
10.0	42.5(1.6)	
5.0	51.2(1.9)	
E_a (kcal/mol)[c]	5.0(1.0)	

[a] The double-jump experiments were carried out by first unfolding from 1.5 M GdnHCl, pH 5.9, to 4.2 M GdnHCl, pH 2.0, and then refolding to 1.5 M GdnHCl, pH 3.0. The final protein concentration was 0.7 mg/mL. The time of unfolding was fixed at 1 s. The numbers in parentheses give the errors at the 95% confidence limit. [b] The double-jump experiments were carried out by first unfolding from 1.5 M GdnHCl, pH 5.9, to 6.0 M GdnHCl, pH 1.9, and then refolding to 1.5 M GdnHCl, pH 3.0. The final protein concentration was 0.5 mg/mL. The time of unfolding was fixed at 1 s. [c] E_a is the activation energy of the rate constants.

that structure because of its fast refolding rate. Such structure would be expected to be destroyed or at least perturbed if a higher GdnHCl concentration (or lower pH) were used for unfolding, therefore affecting the refolding rate and/or the amplitude of U_{vf}. Hence, to check whether U_{vf} is in a completely or partially unfolded state, the double-jump experiments were repeated with the unfolding step carried out at 6 M GdnHCl (instead of 4.2 M) and pH 1.9. The unfolding time was again fixed at 1 s. The rate constants obtained under these new unfolding conditions were the same as those obtained from the 4.2 M GdnHCl unfolding double-jump experiments (Table 4) with the major phase observed (>95%) arising from the refolding of U_{vf}. This result indicates that U_{vf} is *not* a partially unfolded state, i.e., is completely unfolded even at 4.2 M GdnHCl, pH 2.0, and temperatures ≤15 °C (see Discussion section).

The formation of the different unfolded states was monitored by carrying out the double-jump experiments at different unfolding times ranging from ~90 ms to ~2700 s. The protein was unfolded at 4.2 M GdnHCl and pH 2.0; then, after waiting for a specified unfolding time, the protein was refolded at 1.5 M GdnHCl and pH 3.0. The experiments were then repeated using different unfolding times. The refolding event was followed by absorbance at 5, 10, and 15 °C and by fluorescence at 15 °C. The resulting decay curves were fitted to obtain the relative amplitudes $\alpha_{vf}:\alpha_f:\alpha_s$ for the three phases at each unfolding time (Figures 5–7). The three phases correspond to the three unfolded species, U_{vf}, U_f, and U_s, and the relative amplitudes correspond to the relative concentrations of the three species present at that given unfolding time. When the data were fitted to a single or double exponential, only the time constant of the slow phase was fixed (at the values obtained from the single-jump experiments) while all other time constants and amplitudes were allowed to vary. The refolding time constants for U_{vf} and U_f obtained from the double-jump experiments were the same as those obtained from the single-jump refolding experiments within an error of 10%. The total amplitude ($=\alpha_{vf} + \alpha_f + \alpha_s$) as measured by absorbance is constant, within an experimental error of about 15%, at the different unfolding times, indicating that the different unfolded states have the same extinction coefficients. However, the total fluorescence amplitude increases continuously as the unfolding time increases (Figure 7), indicating that the different unfolded species have different quantum yields (see Discussion). From Figures 5 and 7, it can be seen that, as the amplitude of U_{vf} decreases with increasing unfolding time, the amplitudes of U_f and U_s increase; after reaching a certain maximum, the amplitude of U_f decreases toward an equilibrium value. This behavior suggests a sequential mechanism involving U_f.

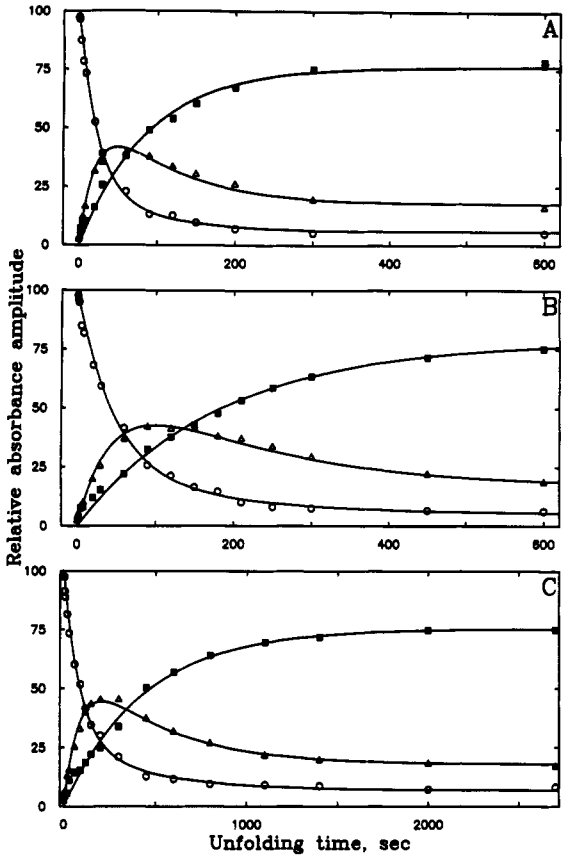

FIGURE 5: The change in the relative absorbance amplitudes of U_{vf} (○), U_f (△), and U_s (■) with time upon unfolding the protein at 4.2 M GdnHCl, pH 2.0: (A) 15 °C, (B) 10 °C, and (C) 5 °C. Double-jump experiments were carried out as follows: RNase A was dissolved in 1.5 M GdnHCl, pH 5.8, and then unfolded at 4.2 M GdnHCl, pH 2.0. After a certain unfolding time, the protein was refolded at 1.5 M GdnHCl, pH 3.0, to obtain the relative amplitudes of the unfolded species. The final protein concentration was 0.7 mg/mL. The solid curves are theoretical fits to the data based on the proposed kinetic model of Figure 8 and the rate constants of Table 5 (see text for discussion). Data for panel B include one additional set of points at 1500 s (beyond the points shown in the plot).

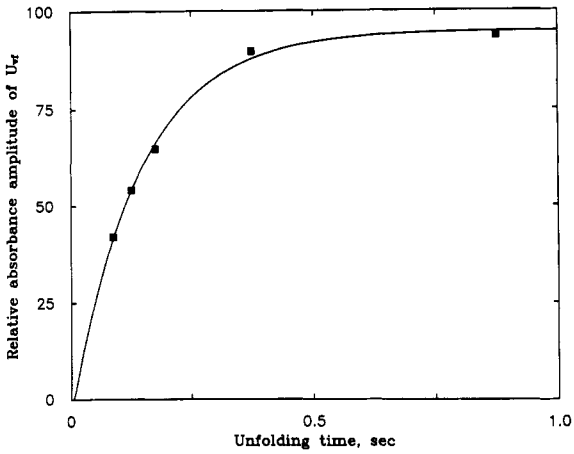

FIGURE 6: The formation of U_{vf} upon unfolding at 4.2 M GdnHCl, pH 2.0, as followed by absorbance at 5 °C. The double-jump experiments are the same as those described for Figure 5. Experimental points (■) show the buildup of U_{vf} at early unfolding times. A single-exponential fit (solid curve) to the experimental points gives τ = 141(±33) ms.

At 5 °C, the unfolding process is sufficiently slow to allow enough points to be obtained at early unfolding times to monitor the formation of U_{vf}. The time constant obtained from fitting the data for the formation of U_{vf} (Figure 6) to a single exponential is τ = 141(±33) ms, and this is the same, within experimental error, as the time constant obtained from the single-jump unfolding experiment under the same conditions [114(±5) ms, Table 1].

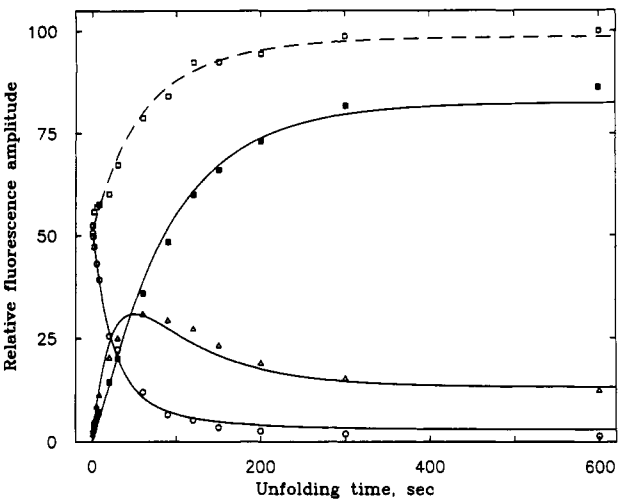

FIGURE 7: The change in the relative fluorescence amplitudes of U_{vf} (○), U_f (△), and U_s (■) with time upon unfolding the protein at 4.2 M GdnHCl, pH 2, and 15 °C. The symbol □ corresponds to the change in the total amplitude (sum of the amplitudes of U_{vf}, U_f, and U_s) with the unfolding time. The double-jump experiments are the same as those described for Figure 5. The solid curves are theoretical fits to the data based on the proposed kinetic model of Figure 8, the 15 °C rate constants of Table 5, and the quantum yield differences of eq 17 (see text for treatment of fluorescence data).

DISCUSSION

In following the refolding or unfolding of a protein by absorbance or fluorescence, the process that is actually being observed is the change in the environment of an aromatic chromophore, e.g., tyrosine in the case of RNase A. Therefore, the actual events that occur as RNase A folds or unfolds cannot be observed directly and can only be inferred by monitoring the changes in the absorbance or fluorescence properties of the tyrosines. By relating these changes to the change in the local or general environment of the chromophore, we can deduce a more detailed picture of the refolding or unfolding events. In general, fluorescence provides a more sensitive probe to the local environment than absorbance (Lakowicz, 1986).

RNase A has three hydrogen-bonded and/or buried tyrosines, Tyr 25, 92, and 97, and three exposed tyrosines, Tyr 73, 76, and 115 (Cha & Scheraga, 1963a,b; Scheraga, 1967; Wlodawer et al., 1988). Tyrosine 25 is part of the second helix, and Tyr 92 is part of a loop region between the two strands of the major β-sheet, while Tyr 97 is part of the β-sheet. Two of these tyrosines are adjacent to prolines which have cis X–Pro peptide bonds in the native state: Tyr 92, which is followed by Pro 93, and Tyr 115, which is preceded by Pro 114. It is known from studies on model peptides of RNase A (Stimson et al., 1982; Montelione et al., 1984; for reviews, see also Nall, 1985; Stein, 1993) and from NMR results (Adler & Scheraga, 1990) that 20–40% of the X–Pro peptide bonds involving Pro 93 and Pro 114 are in a cis conformation and that 60–80% are in a trans conformation when the protein is in its unfolded state. This ability of an X–Pro peptide bond to adopt two conformations is the major cause for the heterogeneity of the unfolded species of RNase A. The activation energy for the cis–trans isomerization process is about 20 kcal/mol (Rehage & Schmid, 1982), and the equilibrium for this isomerization is usually independent

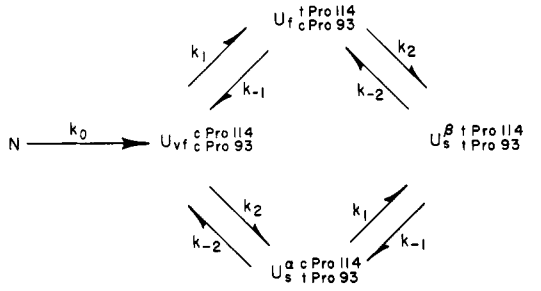

FIGURE 8: Proposed model for the unfolding pathway and interconversion among unfolded species of RNase A at low pH. The model depicts a conformational unfolding step followed by two independent isomerization processes taking place among the unfolded species of the protein at Pro 93 and 114; c and t refer to cis and trans, respectively; U_s^α and U_s^β are two forms of U_s that differ in their conformation at Pro 114. The model is used to fit the data of Figures 5 and 7 (see Discussion for further details).

of temperature, pH, or denaturants in the unfolded state (Schmid & Baldwin, 1978). Therefore, an equilibrium constant of around 3 which is independent of solution conditions and an activation energy of around 20 kcal/mol are good, although not sufficient, indications that the observed process is a proline isomerization.

In the discussion that follows, we use the experimentally obtained activation energies and equilibrium constants to develop and justify a model for the interconversion among unfolded species of RNase A based on proline isomerization (Figure 8).

The Presence of U_{vf}. As presented in the Results section, when the refolding process of RNase A is slowed down, a new phase is observed whose refolding rate is faster than the refolding rate of U_f. Three possible theories can be put forward to explain the presence of this new phase. One explanation is that the new phase results from an intermediate in the refolding pathway of U_f or U_s that has an extinction coefficient and a quantum yield different from those of U_f and U_s. A second explanation is that the unfolding conditions used do not completely denature the protein, giving rise to residual structure in the unfolded state of the protein. This residual structure would then result in the formation of a new species, U_{vf}, which is only partially unfolded and which would, therefore, be expected to refold much faster than U_f. The third explanation is that U_{vf} is a truly unfolded species present in the equilibrium unfolded protein that has not been observed before because of its small refolding amplitude and large refolding rate constant.

From the double-jump experiments, we observe that, upon unfolding from the native protein, U_{vf} is formed before U_f or U_s (Figures 5–7); therefore, U_{vf} is *not* an intermediate in the refolding pathway of U_f or U_s. Also, because of the high GdnHCl concentration and the low pH used for refolding, it is unlikely that any intermediate would be well populated under these conditions. Furthermore, if the protein has some residual structure at 4.2 M GdnHCl and pH 2.0, we would expect such a structure to be at least perturbed, if not completely destroyed, when the GdnHCl concentration is raised to 6 M. The effect of such a perturbation would then be seen in the kinetic behavior of U_{vf} upon refolding either through a change in the time constant and/or through a change in the amplitude. The refolding time constant obtained from the 6 M GdnHCl unfolding double-jump experiments is the same as that obtained from the 4.2 M GdnHCl unfolding double-jump experiments (Table 4), with U_{vf} having the major amplitude. On the basis of this evidence, we conclude that U_{vf} is not a partially unfolded species. As further support that the protein is completely unfolded in 6 M (and hence in 4.2 M) GdnHCl at temperatures of 5–15 °C, Beals et al. (1991) showed that the most hydrophobic portion of RNase A, OT-16 (the last 20 residues in the amino acid sequence of the protein), is essentially unfolded in 6 M GdnHCl at the above temperatures. Also, Salahuddin & Tanford (1970) have shown that RNase A at 4.31 M GdnHCl and pH 6 does not give rise to any thermal transition in the temperature range 5–60 °C and, therefore, can be considered to be a fully denatured protein under these conditions. Hence, U_{vf} is a truly unfolded species lacking any native-like structure (for a review, see Tanford, 1968). The reason that 4.2 M GdnHCl was used rather than 6 M GdnHCl was to reduce the mixing artifacts that appear in the dilution of concentrated GdnHCl buffers.

On the basis of the above arguments, U_{vf} is always present in the equilibrium unfolded protein at low pH and constitutes about 6% of the unfolded species. Hence, the question that arises is, Why was U_{vf} not observed before? One possible explanation is that, when refolding is carried out under strongly native conditions, U_{vf} will have a larger refolding rate constant than that reported here (Table 4), with the same small amplitude. Therefore, under such conditions, the phase due to U_{vf} would be buried in the early mixing events and only the refolding phases involving U_f and U_s would be observed. Alternatively, it is possible that, under such strongly native conditions, U_{vf} and U_f have similar refolding rate constants (on the millisecond time scale) and, therefore, the refolding amplitude reported in the literature for U_f is actually the sum of the amplitudes arising from U_{vf} and U_f, leading to an overestimate of the concentration of U_f in the unfolded state. In either case, it would be difficult to observe U_{vf} under the strongly refolding conditions which have previously been employed in the literature.

Relation between the Refolding Amplitude and Concentration. Before discussion of the proposed kinetic model, it is important to clarify the relation between the refolding amplitudes obtained by absorbance or fluorescence for the different phases and the relative concentrations of the unfolded species that give rise to these phases. The discussion is similar to the treatment of Mui et al. (1985). Since the refolding conditions used in our experiments are unfavorable folding conditions (high GdnHCl and low pH), it is reasonable to assume that there are no well-populated intermediates along the refolding pathway. Furthermore, as in eqs 2–4, each unfolded species is postulated to proceed to the native species along its own pathway. Therefore, the refolding model for a given unfolded species (U) will simply be a two-state process between U and native protein (N):

$$U \xrightarrow{k} N \tag{5}$$

where k is the rate constant of the process. At $t = 0$, U is present with an initial (total) concentration of $[U]_0$. Hence,

$$[U] = [U]_0 e^{-kt} \quad \text{and} \quad [N] = [U]_0(1 - e^{-kt}) \tag{6}$$

If the process is followed by absorbance, then the absorbance, A, at any point along the decay curve would be the sum of the absorbance of the unfolded species A_U and the native species A_N (assume a 1-cm path length):

$$A = A_U + A_N = \epsilon_U[U] + \epsilon_N[N] = [U]_0(\epsilon_U - \epsilon_N)e^{-kt} + [U]_0\epsilon_N \tag{7}$$

where ϵ is the extinction coefficient. Experimentally, the

absorbance refolding data are fitted to an equation of the form

$$A = -\alpha e^{-kt} + \text{constant} \quad (8)$$

where α is the refolding amplitude. Hence, comparing eqs 7 and 8,

$$\alpha = [U]_0(\epsilon_N - \epsilon_U) \quad (9)$$

where $\epsilon_N > \epsilon_U$ for RNase A (Garel et al., 1976). If there are two unfolded species U and U′ that refold to N along their respective pathways, the ratio of their refolding amplitudes would then be

$$\alpha/\alpha' = ([U]_0/[U']_0)(\epsilon_N - \epsilon_U)/(\epsilon_N - \epsilon_{U'}) \quad (10)$$

Therefore, if the extinction coefficients of U and U′ are the same, then the ratio of their refolding amplitudes obtained by absorbance is directly proportional to the ratio of their concentrations. Since the total absorbance amplitude in the double-jump experiments remains unchanged at different unfolding times (as mentioned in the Results section), we conclude that the extinction coefficients of all the unfolded species are approximately the same, which is in agreement with the literature (Garel & Baldwin, 1973; Lin & Brandts, 1983b). Furthermore, in the single-jump unfolding experiments, only one relaxation process was observed (Figure 2A and Table 1), which is expected if all the unfolded species have the same extinction coefficients.

Similarly, when the refolding process is followed by fluorescence, the fluorescence, F, at any point along the decay curve is

$$F = F_U + F_N \quad (11)$$

and

$$F = (\text{constant})I_0QA \quad (12)$$

(Parker & Rees, 1960), where I_0 is the intensity of the exciting light, Q is the quantum yield, and A is the absorbance. Following the same reasoning as that for absorbance, we can write

$$F = (\text{constant})I_0\{[U]_0(Q_U\epsilon_U - Q_N\epsilon_N)e^{-kt} + Q_N\epsilon_N[U]_0\} \quad (13)$$

where $Q_U > Q_N$ for RNase A (Schmid, 1981). The ratio of the fluorescence amplitudes for two unfolded states is then

$$\alpha/\alpha' = ([U]_0/[U']_0)(Q_U\epsilon_U - Q_N\epsilon_N)/(Q_U\epsilon_{U'} - Q_N\epsilon_N) \quad (14)$$

For RNase A, $\epsilon_U = \epsilon_{U'}$ (as discussed above). In addition, the exciting wavelength is usually chosen so that $\epsilon_U = \epsilon_N$. Hence,

$$\alpha/\alpha' = ([U]_0/[U']_0)(Q_U - Q_N)/(Q_{U'} - Q_N) \quad (15)$$

Therefore, for RNase A, the relative amplitudes obtained by fluorescence are equal to the relative concentrations if the quantum yields are the same. However, since the total fluorescence amplitude changes with the unfolding time, as can be seen from Figure 7, then we can conclude that the different unfolded species do not have the same quantum yields. This conclusion is also supported by the fluorescence-detected unfolding experiments where two unfolding phases, rather than one, can be observed. In the subsequent discussion, the quantity $\Delta Q_U = Q_U - Q_N$ will be called the quantum yield difference.

Kinetic Model for the Unfolding Pathway and Interconversion among Unfolded Species. Having established the presence of a new unfolded species (U_{vf}), it is important to be able to describe the nature of that species and its relation to the fast and slow refolding species. Also, it is important to be able to describe the mechanism by which the different unfolded species form from the native protein. Therefore, double-jump experiments were carried out in an effort to deduce a detailed picture for the interconversion among these unfolded species.

The double-jump experiments at 5 °C show the increase in the refolding amplitude of U_{vf} at early unfolding times (Figure 6). As discussed in the previous subsection, the absorbance refolding amplitude of each species is directly proportional to the concentration of that species in the unfolded state; therefore, Figure 6 shows the buildup of $[U_{vf}]$ with the time of unfolding. When the data in Figure 6 are fitted to a single exponential, the time constant obtained is 141(±33) ms, which is the same, within experimental error, as the time constant of 114(±5) ms obtained from the single-jump unfolding experiments (Table 1). The single-jump unfolding experiments monitor the disappearance of the native protein while the double-jump experiments monitor the formation of U_{vf}. Since N is depleted at the same rate at which U_{vf} is formed, as indicated by the above time constants, and since U_{vf} is the only species formed at early unfolding times, we conclude that U_{vf} is the first species to form from the native protein upon unfolding at low pH.

In the refolding kinetics, three phases are observed that result from the presence of at least three species in the unfolded state of RNase A. Furthermore, from the previous discussion, we know that U_{vf} is the first species to form along the unfolding pathway of the protein. Also, from the shapes of the curves in Figures 5 and 7, we can infer that U_f is involved in a sequential mechanism because it builds up and then is depleted. In addition to these observations, it is well established in the literature that the slow phase is actually the sum of at least two phases (Schmid, 1983; Lin & Brandts, 1983b; Lin & Brandts, 1987). On the basis of this information, the simplest model to which the data can be fitted is one that includes two isomerization processes. We propose that these isomerizations occur at the X–Pro peptide bonds of Pro 93 and 114, as will be justified later in this section. Since the isomerizations take place in the unfolded state of the protein and since Pro 93 and 114 are far apart in the amino acid sequence, we will assume that the isomerizations occur independently. Hence, the data were fitted to a *minimal* model for unfolding and interconversion among unfolded species at low pH that includes two independent isomerization processes occurring in the unfolded state. The model represents a general mechanism which is valid as long as two independent isomerizations are taking place in the unfolded state. The model is presented in Figure 8.

In the model (Figure 8), k_0 is the rate constant corresponding to the conformational unfolding step. k_1 and k_{-1} are the rate constants related to the isomerization of Pro 114, while k_2 and k_{-2} are the rate constants related to the isomerization of Pro 93. There are four unfolded species which are distinguished on the basis of the isomeric states of Pro 93 and 114. As discussed in the following subsection, the different isomeric states of Pro 93 and 114 result in the different refolding rates for the unfolded species. U_{vf} is an unfolded species with native proline isomers, while U_f has the wrong Pro 114 isomer. The slow refolding species are those which contain the wrong Pro 93 isomer. There are two slow refolding species; one contains only the wrong Pro 93 isomer (U_s^α), and the other contains both the wrong Pro 93 and the wrong Pro 114 isomers (U_s^β). Experimentally, only the combined two slow phases can be observed under the refolding conditions used, and

Table 5: Fitting the Double-Jump Experiments to the Proposed Unfolding Model[a]

temp (°C)	$(k_1)^{-1}$ (s)	$(k_{-1})^{-1}$ (s)	$(k_2)^{-1}$ (s)	$(k_{-2})^{-1}$ (s)	K_1[b]	K_2[c]
15.0	38(4)	115(24)	116(10)	376(118)	3.05(0.69)	3.25(1.06)
10.0	75(8)	260(71)	232(16)	843(223)	3.47(1.02)	3.64(1.00)
5.0	145(16)	379(122)	577(49)	1773(378)	2.60(0.88)	3.07(0.71)
E_a (kcal/mol)[d]	21.6(2.2)	19.0(5.9)	25.6(1.8)	24.7(5.9)		

[a] Data used are those of Figure 5. Double-jump experiments were carried out by first unfolding from 1.5 M GdnHCl, pH 5.8, to 4.2 M GdnHCl, pH 2.0, and then refolding to 1.5 M GdnHCl, pH 3.0. The final protein concentration was 0.7 mg/mL. The time of unfolding was varied. The rate constants refer to the proposed kinetic model of Figure 8. It should be noted that, in the fitting routine, k_0 was fixed at the values obtained from the single-jump unfolding experiments (Table 1). The numbers in parentheses give the errors at the 95% confidence limit. [b] $K_1 = k_1/k_{-1}$. [c] $K_2 = k_2/k_{-2}$. [d] E_a is the activation energy of the rate constants.

therefore $[U_s] = [U_s^\alpha] + [U_s^\beta]$. The unfolding process first involves the complete unfolding of the native protein and loss of all secondary structure to form the U_{vf} unfolded species. From U_{vf}, there are two possibilities: the isomerization from cis to trans of Pro 93 to form U_s^α or the isomerization from cis to trans of Pro 114 to form U_f. The two isomerizations take place in the unfolded state and are, therefore, considered to be independent of each other. Further isomerizations from U_s^α and U_f will then lead to the formation of U_s^β.

The absorbance data from the double-jump experiments at 5, 10, and 15 °C were fitted to the model of Figure 8, and the best fit curves are shown in Figure 5 (solid lines). The resulting rate constants and activation energies are listed in Table 5. The activation energies for the two independent isomerization processes are around 20 kcal/mol, and the equilibrium ratios (K_1 and K_2 in Table 5) of the nonnative to native conformation are close to 3 and independent of temperature. These numbers justify the conclusion that all the slow processes in the model involve the isomerization of prolines which are cis in the native state, namely, Pro 93 and 114. As mentioned earlier, there is direct NMR evidence (Adler & Scheraga, 1990) that Pro 93 and 114 are 20–40% cis in the unfolded state. On the other hand, the other two prolines, 42 and 117, are trans in the native state and, therefore, their effect on the distribution of unfolded species is expected to be minor. This is further supported by the result of Dodge et al. (1994), who have shown that the Pro-42-Ala mutant has the same distribution of unfolded species as the native protein. Also, there is no direct evidence concerning the ratio of cis to trans conformation for the X–Pro peptide bonds of Pro 42 and 117 in the unfolded state.[2] Hence, for simplicity, any contributions from these two prolines is considered to be minor and is ignored in the kinetic model. It is important to emphasize that, although we propose that the isomerizations which take place are those of the cis prolines, we do not rule out other isomerizations (e.g., those involving disulfide bonds).

Refolding Properties of the Unfolded Species. The different unfolded species of Figure 8 are distinguished on the basis of the conformations of the X–Pro peptide bonds of Pro 93 and 114. These different conformations give rise to the different refolding rates observed for these unfolded species. As mentioned in the introduction, the numerous studies by Baldwin and Schmid indicate that U_s has a nonnative trans Pro 93 isomer which slows down the refolding rate. When refolding is carried out under unfavorable folding conditions (such as those employed in our study), the refolding of U_s is rate-limited by the trans to cis isomerization of Pro 93 resulting in a large time constant for that process and a high activation energy. We report an activation energy of 16 kcal/mol (Table 3) for the refolding of U_s. Furthermore, studies on Ac-Tyr-Pro-Asn-NHMe model peptides (Montelione et al., 1984; Oka et al., 1984) show that, when the Tyr–Pro peptide bond is trans, the peptide cannot adopt a bend conformation due to unfavorable hydrogen bonding. However, when the Tyr–Pro bond is cis, the peptide can adopt a type VI β-bend. Hence, under the unfavorable refolding conditions used here, it seems that the protein has to undergo the trans to cis isomerization of Pro 93 before it folds to the native state. Therefore, under such conditions, any unfolded species with a wrong Pro 93 isomer is expected to be a slow refolding species.

On the other hand, we propose that only Pro 114 is in a nonnative trans conformation in U_f. The activation energy for the folding of U_f is low (6 kcal/mol, Table 3), which indicates that the refolding process is not rate-limited by a proline isomerization. Pro 114 is part of the chain folding initiation site consisting of residues 106–118 (Matheson & Scheraga, 1978; Némethy & Scheraga, 1979), and from theoretical (Pincus et al., 1983; Oka et al., 1984; Ihara & Ooi, 1985) and experimental studies (Stimson et al., 1982; Montelione et al., 1984), it has been demonstrated that this portion of the protein can form a β-turn with the X–Pro peptide bond being in either the cis or trans conformations. As further support of the above proposal, recently, in the Seventh Symposium of the Protein Society held in San Diego, CA (July 24–28, 1993), Schultz et al. (1993) reported the X-ray structure of a cis-proline substitution mutant for RNase A at position 114. The X-ray structure indicates that the peptide bond preceding residue 114 adopts a trans conformation, instead of the wild-type cis conformation, and that the large effects of this change are localized primarily between residues 110 and 117, with the rest of the protein adopting the native conformation. Therefore, the formation of the chain folding initiation site (including the bend) and not the trans to cis isomerization of Pro 114 is expected to be rate-limiting in the refolding of U_f. The low activation energy obtained for the refolding of U_f justifies the conclusion that the rate-determining step is a conformational folding step and not a proline isomerization step. Furthermore, it is reasonable to consider that the rate of formation of the chain folding initiation site may be slower if the Asn 113–Pro 114 peptide bond is in the nonnative trans conformation than if it is in the native cis conformation. Therefore, the fact that the refolding rate of U_{vf}, in which Pro 114 is cis, is faster than that of U_f, in which Pro 114 is trans, is consistent with our proposed model (Figure 8).

The Nature of U_s^I and U_s^{II}. In the proposed kinetic model of Figure 8, there are two slow folding species (U_s^α and U_s^β) whose refolding phases are not kinetically resolved under the unfavorable folding conditions used in our experiments,

[2] By using isomer-specific proteolysis (ISP), Lin and Brandts (1984) have estimated that Pro 117 is 100% trans in the unfolded state. However, results obtained by this method for Pro 93 and 114 (Lin & Brandts, 1983a, 1984) do not agree with the NMR results of Adler and Scheraga (1990). By ISP, 70% of Pro 93 and 95% of Pro 114 were found to adopt the cis conformation in the unfolded state, while, by NMR, the percentages were found to be 40% and 37%, respectively.

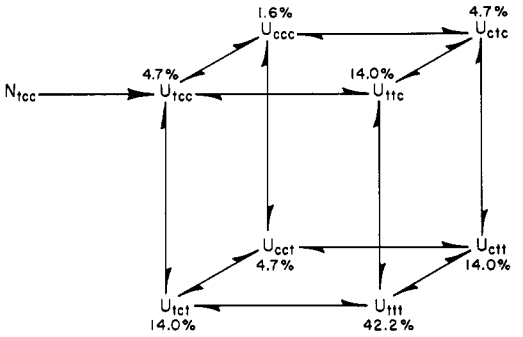

FIGURE 9: A kinetic model for the case in which RNase A has to undergo three isomerizations in its unfolded state. Two isomerization processes occur at the X–Pro peptide bonds of Pro 93 and 114 which are cis in the native state, while the third isomerization occurs at some unknown site which is labeled as trans when in the native conformation and as cis when in the nonnative conformation. The subscripts refer to the conformation at the third site, at Pro 93, and at Pro 114, respectively, in that sequence. The numbers next to each species refer to the relative concentration of that species in the unfolded state calculated by assuming that the trans to cis ratio in the unfolded state for each of the three isomerizations is 3.

where both phases are presumably rate-limited by the isomerization process of Pro 93. However, if the refolding experiments are carried out under strongly native folding conditions, two distinct slow folding phases, corresponding to the unfolded species U_s^I and U_s^{II}, can be observed experimentally (Schmid, 1981).

If we consider that the average value of the equilibrium constants for the isomerization processes described in the model of Figure 8 is around 3 (i.e., in Table 5, $K_1 = K_2 = 3$, independent of temperature), then the relative concentrations of the unfolded species at equilibrium would be

$$[U_{vf}]:[U_f]:[U_s^\alpha]:[U_s^\beta] = 6.25:18.75:18.75:56.25 \quad (16)$$

The ratio $[U_s^\alpha]:[U_s^\beta] = 25:75$ is close to the value of $[U_s^I]:[U_s^{II}]$ [Schmid (1981) reports a ratio of about 20:80]. We have also carried out the single-jump refolding experiments under conditions where U_s^I and U_s^{II} can be observed and found a ratio of $[U_s^I]:[U_s^{II}] = 22:78$ (W. A. Houry & H. A. Scheraga, unpublished results). Experimentally, the major species U_s^{II} folds *faster* than the minor species U_s^I; however, in the proposed kinetic model, the major species U_s^β has two wrong prolines and, therefore, would be expected to fold *slower* than the minor species U_s^α, which has only one wrong proline isomer.

There are two possible explanations for the above result. The first would be the presence of a third *essential* isomerization process that was not taken into account in the model of Figure 8 and which is "transparent" under the conditions of our experiments. The ratio of the concentration of the native to the nonnative conformation of this third unknown isomerization process would have to be about 3:1 in the unfolded state to obtain the expected equilibrium concentration for the U_s^I species. This species, being the slowest to fold, would contain three wrong isomers. Figure 9 shows an example of a kinetic model in which the protein has to undergo three isomerizations in its unfolded state. In this model, two of the isomerizations occur at the X–Pro peptide bonds of Pro 93 and 114, while the third isomerization occurs at a third unknown site. The native conformation of the bond causing the third isomerization is labeled as "trans" and the nonnative as "cis" for reasons which will be made clear in the following paragraph. On the basis of this model, the species U_{tcc}, which has all the correct isomers, would correspond to U_{vf}, while U_{tct}, which has the wrong Pro 114 isomer, would correspond to U_f. U_{ccc}, which has the wrong isomer at the third unknown site, would correspond to a very fast or a fast folding species. U_{cct}, which has the wrong isomer at the third unknown site and the wrong isomer at Pro 114, would correspond to a fast folding species or, alternatively, to a species with a folding rate intermediate between fast and slow. As in the previous model of Figure 8, the slow refolding species are those that have Pro 93 in the wrong conformation. There are four such species: U_{ctt}, U_{ctc}, U_{ttc}, and U_{ttt}, which are present at the corners of the right face of the box of Figure 9. U_{ctt}, which is the species with three wrong isomers, would correspond to the slower refolding species U_s^I. The other three species (U_{ctc}, U_{ttc}, and U_{ttt}) would, therefore, correspond to U_s^{II}. The ratio $[U_{ctt}]:([U_{ctc}] + [U_{ttc}] + [U_{ttt}]) = 19:81$ is similar to the experimentally determined value of $[U_s^I]:[U_s^{II}]$ under strongly native folding conditions. In this model, the isomerization process at the third unknown site, as in the case of the isomerization process at Pro 114, is for the most part silent under both weakly and strongly native folding conditions. Its only observable contribution would be to the refolding kinetics of the unfolded species which contains all three wrong isomers (U_{ctt}).

A possible origin of this third isomerization process is the involvement of one of the trans prolines: Pro 42 or 117. However, recent studies in this laboratory on a Pro 42 mutant indicate that the kinetics of the Pro-42-Ala mutant do not change significantly when compared to the kinetics of the native protein (Dodge et al., 1994). This then leaves Pro 117 as a likely candidate. Disulfide bond isomerization is another possibility for the origin of the third isomerization process. However, little is known about the chirality of the disulfide bonds in the unfolded state, or the value of the activation energy for interconversion between a left-handed disulfide bond and a right-handed one. Therefore, this possibility cannot be verified. It is worth mentioning at this point that Otting et al. (1993) have recently been able to detect two conformations for the Cys 14–Cys 38 disulfide bond in native BPTI, and they were able to estimate an activation energy of around 10 kcal/mol for the disulfide flip process in the native protein. However, their result cannot be generalized to other proteins in their unfolded states. Mui et al. (1985) have suggested that the activation energy for disulfide bond isomerization in globular proteins may contain a contribution due to steric hindrance and, therefore, might be sequence dependent.

A second possible explanation is that U_s^α and U_s^β are the same as U_s^I and U_s^{II}, respectively, and, therefore, the unfolded species with two wrong proline isomers actually folds faster than the unfolded species with one wrong proline isomer due to some cooperativity between the two prolines during the refolding process. This cooperativity could be due to some steric or energetic requirement for the trans to cis isomerization of Pro 93 as the formation of the sheet region proceeds during the refolding process. This cooperativity can be explained on the basis of the premise that a nonnative trans conformation at Pro 114 can cause enough perturbation in the neighboring β-sheet to allow the protein to adopt, upon folding, a native-like structure while both Pro 93 and 114 are still in their nonnative trans conformations. This explains the presence of I_N, the native-like intermediate in the refolding pathway of U_s^{II} under strongly native folding conditions, which would have both Pro 93 and 114 in a nonnative trans conformation according to the above premise. Furthermore, Cook et al. (1979) have shown experimentally that proline isomerization is faster in I_N than in unfolded RNase A. Therefore, after

native-like structure is formed in I_N, presumably with Pro 114 still in the trans conformation, Pro 93 isomerizes quickly to the cis conformation "catalyzed" by the presence of that native-like structure. On the basis of this "proline coupling" explanation, the sequence of events during the refolding of U_s^{II} (U_s^{β}) under strongly native conditions would involve the formation of native-like structure followed by the isomerization of Pro 93 from trans to cis and then (or concurrently) the isomerization of Pro 114 from trans to cis. On the other hand, when the chain folding initiation site (104–118) is formed with a cis Pro 114, as is the case for U_s^{α}, there is no structural perturbation in the region after Pro 93 and, therefore, the protein cannot attain the native structure unless Pro 93 isomerizes to the cis conformation. Hence, the folding of U_s^{α} (U_s^{I}) would be rate-limited by the isomerization of Pro 93 leading to its slower refolding rate than U_s^{β} (U_s^{II}).

Further insight into the contributions of the prolines to the refolding and the unfolding kinetics of RNase A will probably come from mutants with unnatural amino acids that are able to "lock" the X–Pro peptide bond in the cis conformation whether the protein is in its folded or unfolded state(s), thereby simplifying the kinetics.

Fluorescence Properties of the Unfolded Species. The absorbance and fluorescence double-jump experiments monitor the same process, namely, the formation of the different unfolded species from the native protein as described in the model of Figure 8. However, as indicated by eq 15, the fluorescence refolding amplitude for each species is not proportional to the concentration of that species, but rather to the product of the concentration and the quantum yield difference of that species. Therefore, in fitting the fluorescence refolding amplitudes obtained from the fluorescence double-jump experiments at 15 °C, the relative concentrations of the unfolded states $[U_{vf}]$:$[U_f]$:$[U_s^{\alpha}]$:$[U_s^{\beta}]$ were generated using the model of Figure 8 and the rate constants (k_1, k_{-1}, k_2, and k_{-2}) obtained from the double-jump absorbance data at 15 °C (Table 5). The values of the quantum yield differences were varied (using the Simplex algorithm) until a best fit to the fluorescence amplitudes was found (Figure 7, solid curves). The following relative values were obtained for the quantum yield differences at 1.5 M GdnHCl, pH 3.0, and 15 °C:

$$\Delta Q_{vf}:\Delta Q_f:\Delta Q_s^{\alpha}:\Delta Q_s^{\beta} = 42.4(1.0):61.2(1.8):56.3(4.9):100.0(2.5) \quad (17)$$

The numbers in parentheses are the errors at the 95% confidence limit.

It should be noted that the unfolded species U_f and U_s^{α}, which are each proposed to contain one wrong proline isomer, have similar quantum yields. However, it would be difficult to interpret the results on a molecular level because of the subtle nature of the fluorescence quenching mechanisms. Since Tyr 92 precedes Pro 93 while Tyr 115 follows Pro 114, the fluorescence of each tyrosine is expected to be affected differently by the conformation of the X–Pro peptide bond. Nevertheless, it seems that both tyrosines are quenched to a similar extent when the X–Pro peptide bond is in the cis conformation. Haas et al. (1987) have used fluorescence lifetime measurements to study the effects of the conformation of the X–Pro peptide bond on the fluorescence of a nearby tyrosine. For Tyr-Pro-containing peptides, the lifetime decay curves obtained were biexponential and the ratios of the preexponential factors were proportional to the relative amplitudes of the cis to trans conformations as measured by NMR spectroscopy. However, for the OT-16 fragment (residues 105–124), which contains the Pro-Tyr sequence, the relative amplitudes obtained from the lifetime measurements did not correlate with the relative amplitudes obtained by NMR spectroscopy for the cis and trans conformations present in that fragment around the Asn–Pro peptide bond.

Using the values in eq 17, it can be seen that the change in the quantum yield when Pro 93 isomerizes from the cis to the trans conformation is 56 – 42 = 14, and the change due to the isomerization of Pro 114 is 61 – 42 = 19. Therefore, if the contributions from the isomerization of the two prolines are additive, then ΔQ_s^{β} is expected to be 42 + 14 + 19 = 75 when the two prolines are trans. This value does not agree with the experimental value of 100. A possible explanation is that, if one tyrosine in the protein is quenched, the fluorescence of the other tyrosines may be reduced through a fluorescence energy transfer process (Edelhoch et al., 1968; Bent & Hayon, 1975), as was observed, e.g., in RNase A with iodinated tyrosyl residues (Cowgill, 1965). Another possible explanation is that a more complicated model, like the one presented in Figure 9, has to be considered in order to interpret the fluorescence data properly.

Relaxation Rates for the Unfolding Process. In the single-jump unfolding experiments, only one phase is observed when the process is monitored by absorbance. This is a consequence of the fact that all the unfolded states have nearly identical extinction coefficients and, therefore, only the first conformational unfolding step from N to U_{vf} can be observed. However, when the unfolding process is monitored by fluorescence, two phases are observed: one corresponds to the phase detected by absorbance while the other is a much slower phase (Table 1 and Figure 2). By using the proposed kinetic model of Figure 8 and the calculated quantum yield differences (eq 17), we should be able to explain the two phases observed by fluorescence single-jump unfolding. This would provide an independent test for the validity of our model and the reliability of the values obtained for the quantum yield differences of the different unfolded species.

In order to understand the origin of the relaxations observed in the single-jump unfolding experiments, we will consider the data obtained at 15 °C. The proposed model of Figure 8 consists of five species; therefore, theoretically, there are four relaxation rates (or apparent rate constants) (Bernasconi, 1976) that describe the approach of each species to its equilibrium value. The rate equations can be described by a set of four independent first-order differential equations. The equations were solved analytically following the procedure of Benson (1960) (see Appendix). It can be shown (see Appendix) that, for the model of Figure 8, the fluorescence unfolding signal is proportional to

$$F \propto -42e^{-\lambda_1 t} - 25e^{-\lambda_2 t} - 29e^{-\lambda_3 t} + 14e^{-\lambda_4 t} + \text{constant} \quad (18)$$

where the λ's refer to the relaxation rates and are related to the rate constants of Figure 8 by

$$\begin{aligned} \lambda_1 &= k_0 = 28.57\ s^{-1} \\ \lambda_2 &= k_2 + k_{-2} = 0.0113\ s^{-1} \\ \lambda_3 &= k_1 + k_{-1} = 0.0353\ s^{-1} \\ \lambda_4 &= k_1 + k_{-1} + k_2 + k_{-2} = 0.0466\ s^{-1} \end{aligned} \quad (19)$$

The numbers given are those from the double-jump data at 1.5 M GdnHCl, pH 3.0, and 15 °C.

A negative amplitude in eq 18 indicates an increasing fluorescence signal while a positive amplitude indicates a decreasing fluorescence signal. Equation 19 defines the

different processes that give rise to the four relaxations. λ_1 relaxation corresponds to the conformational unfolding step during which U_{vf} is formed from N, and since $Q_{vf} > Q_N$, the process is observed as an increase in the fluorescence signal. λ_2 relaxation corresponds to the Pro 93 isomerization steps during which U_s^α is formed from U_{vf} and U_s^β is formed from U_f, and since $Q_s^\alpha > Q_{vf}$ and $Q_s^\beta > Q_f$, the process is also observed as an increase in the fluorescence signal. The λ_3 relaxation corresponds to the Pro 114 isomerization during which U_f is formed from U_{vf}, and U_s^β is formed from U_s^α, and since $Q_f > Q_{vf}$ and $Q_s^\beta > Q_s^\alpha$, the process is observed as an increase in the fluorescence signal. Finally, λ_4 is a relaxation corresponding to a rate constant describing the two isomerization processes simultaneously whereby (U_f and U_s^α) are formed from (U_{vf} and U_s^β). Since $Q_f + Q_s^\alpha < Q_{vf} + Q_s^\beta$, the process is seen as a decrease in the fluorescence signal.

Hence, the fast phase observed experimentally by fluorescence upon unfolding corresponds to the λ_1 relaxation, which is the conformational unfolding step to form U_{vf}, while the slow phase corresponds to the sum of exponentials $-25e^{-\lambda_2 t} - 29e^{-\lambda_3 t} + 14e^{-\lambda_4 t}$. Since λ_2, λ_3, and λ_4 are of approximately the same magnitude, it will be difficult to deconvolute their sum. Upon fitting the sum to a single exponential, a value of 67 s is obtained for the apparent time constant, which is in close agreement with the value of 70 s obtained experimentally (Table 1) for the slow unfolding phase. Since λ_3 and λ_4 have similar values and since their respective amplitudes are of opposite signs, they are expected to cancel each other partially. Therefore, the major contribution to the slow unfolding phase comes from the λ_2 relaxation, which corresponds to the isomerization process of Pro 93. Unfortunately, the amplitudes obtained from the single-jump unfolding experiments cannot be compared directly to the amplitudes obtained from the above analysis because the absolute quantum yield of the native species (but not the relative quantum yields of the unfolded species) is expected to be affected by the solution conditions used: 4.2 M GdnHCl, pH 2.0 for single-jump unfolding experiments, and 1.5 M GdnHCl, pH 3.0 for the double-jump experiments.

Therefore, the fluorescence unfolding experiments support the model of Figure 8 and indicate that the values obtained for the quantum yield differences are reasonable.

Transient Intermediate Observed Previously in the Unfolding of RNase A. In the literature, an early unfolding intermediate labeled I_3 has been reported to exist upon unfolding at low pH (Hagerman et al., 1979; Rehage & Schmid, 1982). Hagerman et al. were able to detect that intermediate by using double-jump experiments at 47 °C using pH 2.0 for unfolding and pH 5.8 for refolding. No denaturants were used in their study. Furthermore, the authors estimate that I_3 makes up less than 2% of the species present at equilibrium (compared to ~6% for U_{vf}). Little is known about the nature of I_3, and therefore, we can only speculate that I_3 and U_{vf} might be the same species since both can be detected upon unfolding at low pH and both constitute a small percentage of the equilibrium unfolded state.

CONCLUSION

By slowing the refolding process of RNase A, a new very fast folding phase has been detected in addition to the usual fast and slow phases. The new phase arises from a separate unfolded species, which we have labeled U_{vf}. A new model for the interconversion among unfolded species is proposed which is based on the presence of two independent isomerization processes: one at Pro 93 and the other at Pro 114. Analysis of the kinetic data based on the new model indicates that both prolines are in their native conformation in U_{vf}, that Pro 114 is in the nonnative conformation in U_f, and that at least Pro 93 is in the nonnative conformation in the slow folding species (U_s). Although both isomerizations about Pro 93 and 114 are proposed to give rise to the unfolded species, only the cis–trans isomerization of Pro 93 is suggested to be rate-limiting in the refolding of RNase A.

ACKNOWLEDGMENT

Thanks are due to R. W. Dodge and D. R. Buckler for their many comments and helpful discussions during the course of this project. We also thank V. G. Davenport for technical assistance.

APPENDIX

Derivation of the Fluorescence Unfolding Signal (Eq 18). The integrated rate equations for the five species in the kinetic model of Figure 8 were derived on the basis of the procedure of Benson (1960) for solving a set of first-order differential equations. The differential equations are

$$d[N]/dt = -k_0[N]$$

$$d[U_{vf}]/dt = k_0[N] - (k_1 + k_2)[U_{vf}] + k_{-1}[U_f] + k_{-2}[U_s^\alpha]$$

$$d[U_f]/dt = k_1[U_{vf}] - (k_{-1} + k_2)[U_f] + k_{-2}[U_s^\beta] \quad \text{(A-1)}$$

$$d[U_s^\alpha]/dt = k_2[U_{vf}] - (k_1 + k_{-2})[U_s^\alpha] + k_{-1}[U_s^\beta]$$

$$d[U_s^\beta]/dt = k_2[U_f] + k_1[U_s^\alpha] - (k_{-1} + k_{-2})[U_s^\beta]$$

The integrated rate equations for the 15 °C absorbance double-jump data are

$$\begin{array}{lcllll} [N] & = & e^{-\lambda_1 t} & +0 & +0 & +0 \\ [U_{vf}] & = & -e^{-\lambda_1 t} & +0.189e^{-\lambda_2 t} & +0.177e^{-\lambda_3 t} & +0.576e^{-\lambda_4 t} \quad +0.058 \\ [U_f] & = & 0 & +0.576e^{-\lambda_2 t} & -0.177e^{-\lambda_3 t} & -0.576e^{-\lambda_4 t} \quad +0.177 \\ [U_s^\alpha] & = & 0 & -0.189e^{-\lambda_2 t} & +0.576e^{-\lambda_3 t} & -0.576e^{-\lambda_4 t} \quad +0.189 \\ [U_s^\beta] & = & 0 & -0.576e^{-\lambda_2 t} & -0.576e^{-\lambda_3 t} & +0.576e^{-\lambda_4 t} \quad +0.576 \end{array} \quad \text{(A-2)}$$

The λ's are the relaxation rates as defined in the text (see Discussion section, eq 19). The equations satisfy the mass conservation expression

$$[N]_0 = [N] + [U_{vf}] + [U_f] + [U_s^\alpha] + [U_s^\beta] = 1 \quad \text{(A-3)}$$

where $[N]_0$ is the initial concentration of the native protein.

The curves for U_{vf}, U_f, and $U_s = U_s^\alpha + U_s^\beta$ are the same as the solid curves plotted in Figure 5A (after multiplying by a factor of 100). The constants in the above expressions represent the concentrations of the respective species at infinite time when the system reaches equilibrium in the unfolding direction.

Similar to the expression of eq 11 in the Discussion section, the total observed fluorescence unfolding signal can be written as

$$F = F(N) + F(U_{vf}) + F(U_f) + F(U_s^\alpha) + F(U_s^\beta) \quad \text{(A-4)}$$

By using eq 12, the total fluorescence signal is proportional to

$$F \propto Q(N)\,A(N) + Q(U_{vf})\,A(U_{vf}) + Q(U_f)\,A(U_f) + Q(U_s^\alpha)\,A(U_s^\alpha) + Q(U_s^\beta)\,A(U_s^\beta) \quad \text{(A-5)}$$

where Q is the quantum yield and A is the absorbance. Since $A = \epsilon bc$, where ϵ is the extinction coefficient, b is the cell path

length (taken as 1 cm), and c is the concentration, we can write

$$F \propto Q(N)\,\epsilon(N)\,[N] + Q(U_{vf})\,\epsilon(U_{vf})\,[U_{vf}] + Q(U_f)\,\epsilon(U_f)\,[U_f] + Q(U_s^{\alpha})\,\epsilon(U_s^{\alpha})\,[U_s^{\alpha}] + Q(U_s^{\beta})\,\epsilon(U_s^{\beta})\,[U_s^{\beta}] \quad \text{(A-6)}$$

The concentrations for each species are the time-dependent concentrations listed above (eqs A-2). From the Discussion section, we have seen that $\epsilon(U_{vf}) = \epsilon(U_f) = \epsilon(U_s^{\alpha}) = \epsilon(U_s^{\beta}) = \epsilon(U)$. Furthermore, the excitation wavelength is chosen so that $\epsilon(N) = \epsilon(U)$. Therefore,

$$F \propto \{Q(N) - Q(U_{vf})\}e^{-\lambda_1 t} + \{0.189[Q(U_{vf}) - Q(U_s^{\alpha})] + 0.576[Q(U_f) - Q(U_s^{\beta})]\}e^{-\lambda_2 t} + \{0.177[Q(U_{vf}) - Q(U_f)] + 0.576[Q(U_s^{\alpha}) - Q(U_s^{\beta})]\}e^{-\lambda_3 t} + \{0.576[Q(U_{vf}) - Q(U_f) - Q(U_s^{\alpha}) + Q(U_s^{\beta})]\}e^{-\lambda_4 t} + \text{constant} \quad \text{(A-7)}$$

By substituting the values obtained for the quantum yield differences (eq 17) into eq A-7, we obtain

$$F \propto -42e^{-\lambda_1 t} - 25e^{-\lambda_2 t} - 29e^{-\lambda_3 t} + 14e^{-\lambda_4 t} + \text{constant} \quad \text{(A-8)}$$

which is the same as eq 18.

REFERENCES

Adler, M., & Scheraga, H. A. (1990) *Biochemistry 29*, 8211–8216.

Anfinsen, C. B., & Scheraga, H. A. (1975) *Adv. Protein Chem. 29*, 205–300.

Armstrong, J. McD. (1964) *Biochim. Biophys. Acta 86*, 194–197.

Beals, J. M., Haas, E., Krausz, S., & Scheraga, H. A. (1991) *Biochemistry 30*, 7680–7692.

Benson, S. W. (1960) *The Foundations of Chemical Kinetics*, Chapter 3, pp 39–42, McGraw-Hill Book Company, New York.

Bent, D. V., & Hayon, E. (1975) *J. Am. Chem. Soc. 97*, 2599–2606.

Bernasconi, C. F. (1976) *Relaxation Kinetics*, *Chapter* 3, p 20, Academic Press, New York.

Brandts, J. F., Halvorson, H. R., & Brennan, M. (1975) *Biochemistry 14*, 4953–4963.

Brems, D. N., & Baldwin, R. L. (1985) *Biochemistry 24*, 1689–1693.

Caceci, M. S., & Cacheris, W. P. (1984) *BYTE 9*, 340–362.

Cha, C.-Y., & Scheraga, H. A. (1963a) *J. Biol. Chem. 238*, 2958–2964.

Cha, C.-Y., & Scheraga, H. A. (1963b) *J. Biol. Chem. 238*, 2965–2975.

Cook, K. H., Schmid, F. X., & Baldwin, R. L. (1979) *Proc. Natl. Acad. Sci. U.S.A. 76*, 6157–6161.

Cowgill, R. W. (1965) *Biochim. Biophys. Acta 94*, 74–80.

Denton, J. B., Konishi, Y., & Scheraga, H. A. (1982) *Biochemistry 21*, 5155–5163.

Dodge, R. W., Laity, J. H., Rothwarf, D. M., Shimotakahara, S., & Scheraga, H. A. (1994) *J. Protein Chem.* (submitted).

Dyson, H. J., Rance, M., Houghten, R. A., Lerner, R. A., & Wright, P. E. (1988) *J. Mol. Biol. 201*, 161–200.

Edelhoch, H., Perlman, R. L., & Wilchek, M. (1968) *Biochemistry 7*, 3893–3900.

Garel, J.-R., & Baldwin, R. L. (1973) *Proc. Natl. Acad. Sci. U.S.A. 70*, 3347–3351.

Garel, J.-R., & Baldwin, R. L. (1975) *J. Mol. Biol. 94*, 611–620.

Garel, J.-R., Nall, B. T., & Baldwin, R. L. (1976) *Proc. Natl. Acad. Sci. U.S.A. 73*, 1853–1857.

Good, N. E., & Izawa, S. (1972) *Methods Enzymol. 24*, 53–68.

Haas, E., Montelione, G. T., McWherter, C. A., & Scheraga, H. A. (1987) *Biochemistry 26*, 1672–1683.

Hagerman, P. J., & Baldwin, R. L. (1976) *Biochemistry 15*, 1462–1473.

Hagerman, P. J., Schmid, F. X., & Baldwin, R. L. (1979) *Biochemistry 18*, 293–297.

Henkens, R. W., Gerber, A. D., Cooper, M. R., & Herzog, W. R., Jr. (1980) *J. Biol. Chem. 255*, 7075–7078.

Ihara, S., & Ooi, T. (1985) *Biochim. Biophys. Acta 830*, 109–112.

Jaenicke, R. (1987) *Prog. Biophys. Mol. Biol. 49*, 117–237.

Kim, P. S., & Baldwin, R. L. (1980) *Biochemistry 19*, 6124–6129.

Kim, P. S., & Baldwin, R. L. (1990) *Annu. Rev. Biochem. 59*, 631–660.

Krebs, H., Schmid, F. X., & Jaenicke, R. (1983) *J. Mol. Biol. 169*, 619–635.

Lakowicz, J. R. (1986) *Principles of Fluorescence Spectroscopy*, Chapter 11, pp 341–379, Plenum Press, New York.

Lang, K., & Schmid, F. X. (1990) *J. Mol. Biol. 212*, 185–196.

Lang, K., Wrba, A., Krebs, H., Schmid, F. X., & Beintema, J. J. (1986) *FEBS Lett. 204*, 135–139.

Lin, L.-N., & Brandts, J. F. (1983a) *Biochemistry 22*, 559–563.

Lin, L.-N., & Brandts, J. F. (1983b) *Biochemistry 22*, 564–573.

Lin, L.-N., & Brandts, J. F. (1983c) *Biochemistry 22*, 573–580.

Lin, L.-N., & Brandts, J. F. (1984) *Biochemistry 23*, 5713–5723.

Lin, L.-N., & Brandts, J. F. (1987) *Biochemistry 26*, 3537–3543.

Marquardt, D. W. (1963) *J. Soc. Ind. Appl. Math. 11*, 431–441.

Matheson, R. R., Jr., & Scheraga, H. A. (1978) *Macromolecules 11*, 819–829.

Montelione, G. T., Arnold, E., Meinwald, Y. C., Stimson, E. R., Denton, J. B., Huang, S.-G., Clardy, J., & Scheraga, H. A. (1984) *J. Am. Chem. Soc. 106*, 7946–7958.

Mui, P. W., Konishi, Y., & Scheraga, H. A. (1985) *Biochemistry 24*, 4481–4489.

Nall, B. T. (1985) *Comments Mol. Cell. Biophys. 3*, 123–143.

Nall, B. T., Garel, J.-R., & Baldwin, R. L. (1978) *J. Mol. Biol. 118*, 317–330.

Nelder, J. A., & Mead, R. (1965) *Comput. J. 7*, 308–313.

Némethy, G., & Scheraga, H. A. (1979) *Proc. Natl. Acad. Sci. U.S.A. 76*, 6050–6054.

Nozaki, Y. (1972) *Methods Enzymol. 26*, 43–50.

Oka, M., Montelione, G. T., & Scheraga, H. A. (1984) *J. Am. Chem. Soc. 106*, 7959–7969.

Otting, G., Liepinsh, E., & Wüthrich, K. (1993) *Biochemistry 32*, 3571–3582.

Parker, C. A., & Rees, W. T. (1960) *Analyst (London) 85*, 587–600.

Pincus, M. R., Gerewitz, F., Wako, H., & Scheraga, H. A. (1983) *J. Protein Chem. 2*, 131–146.

Rehage, A., & Schmid, F. X. (1982) *Biochemistry 21*, 1499–1505.

Richards, F. M., & Wyckoff, H. W. (1971) *Enzymes 4*, 647–806.

Rothwarf, D. M., & Scheraga, H. A. (1993) *Biochemistry 32*, 2671–2679.

Salahuddin, A., & Tanford, C. (1970) *Biochemistry 9*, 1342–1347.

Scheraga, H. A. (1967) *Fed. Proc. 26*, 1380–1387.

Schmid, F. X. (1981) *Eur. J. Biochem. 114*, 105–109.

Schmid, F. X. (1982) *Eur. J. Biochem. 128*, 77–80.

Schmid, F. X. (1983) *Biochemistry 22*, 4690–4696.

Schmid, F. X. (1986) *Methods Enzymol. 131*, 70–82.

Schmid, F. X., & Baldwin, R. L. (1978) *Proc. Natl. Acad. Sci. U.S.A. 75*, 4764–4768.

Schmid, F. X., & Baldwin, R. L. (1979a) *J. Mol. Biol. 133*, 285–287.

Schmid, F. X., & Baldwin, R. L. (1979b) *J. Mol. Biol. 135*, 199–215.

Schmid, F. X., & Blaschek, H. (1981) *Eur. J. Biochem. 114*, 111–117.

Schmid, F. X., Grafl, R., Wrba, A., & Beintema, J. J. (1986) *Proc. Natl. Acad. Sci. U.S.A. 83*, 872–876.
Schultz, D. A., & Baldwin, R. L. (1992) *Protein Sci. 1*, 910–916.
Schultz, D. A., Schmid, F. X., & Baldwin, R. L. (1992) *Protein Sci. 1*, 917–924.
Schultz, D. A., Friedman, A., & Fox, R. O. (1993) *Protein Sci. 2*, Suppl. 1, p 67, Abstract No. 66-M.
Sela, M., & Anfinsen, C. B. (1957) *Biochim. Biophys. Acta 24*, 229–235.
Stein, R. L. (1993) *Adv. Protein Chem. 44*, 1–24.
Stimson, E. R., Montelione, G. T., Meinwald, Y. C., Rudolph, R. K. E., & Scheraga, H. A. (1982) *Biochemistry 21*, 5252–5262.
Straume, M., & Johnson, M. L. (1992) *Methods Enzymol. 210*, 117–129.
Tanford, C. (1968) *Adv. Protein Chem. 23*, 121–282.
Thomas, W. A., & Williams, M. K. (1972) *J. Chem. Soc., Chem. Commun. 17*, 994.
Tonomura, B., Nakatani, H., Ohnishi, M., Yamaguchi-Ito, J., & Hiromi, K. (1978) *Anal. Biochem. 84*, 370–383.
Udgaonkar, J. B., & Baldwin, R. L. (1988) *Nature (London) 335*, 694–699.
Udgaonkar, J. B., & Baldwin, R. L. (1990) *Proc. Natl. Acad. Sci. U.S.A. 87*, 8197–8201.
Wlodawer, A., & Sjölin, L. (1983) *Biochemistry 22*, 2720–2728.
Wlodawer, A., Svensson, L. A., Sjölin, L., & Gilliland, G. L. (1988) *Biochemistry 27*, 2705–2717.
Wüthrich, K., & Grathwohl, C. (1974) *FEBS Lett. 43*, 337–340.